Table III. Photochemical Decomposition of Tetrahydrothiophene (THT) under Aerobic Conditions Catalyzed by Various Catalysts[a]

catalyst	mole ratio[b]	% decompn[c]
Polyoxometalate Systems		
$Q_4W_{10}O_{32}$	20	~100
$Q_3PMo_{12}O_{40}$	10	<1
$Q_3PW_{12}O_{40}$	10	0
$Q_4SiMo_{12}O_{40}$	10	8
$Q_5PV_2Mo_{10}O_{40}$	10	7
$H_5PV_2Mo_{10}O_{40}$	10	46
$Q_5Cu^{II}W_{11}PO_{39}$	10	12
$(NH_4)_6P_2W_{18}O_{62}$	10	12
Semiconductor Systems		
TiO_2 (Degussa)	1	80
TiO_2 (Degussa)	2	63
TiO_2	1	35
TiO_2	2	26
SnO_2	1	10
WO_3	1	0
CdS	1	0

[a] Irradiation time in all cases 4 h; source 1000-W Xe arc lamp with 340-nm cutoff and circulating infrared water filters (see Experimental Section); reactions were run in 5 mL of CH_3CN in 30-mL Schlenk flasks. [b] mol of THT/mol of photocatalyst (either polyoxometalate or semiconductor). [c] $(1 - [R_2S]_{end}/[R_2S]_0) \times 100$, where $[R_2S]_{end}$ = quantity of thioether after irradiation; 0% means products below the detectable limit (yield <2%).

compounds under similar conditions.[1d,2d] It is not surprising that the reactivities of the different semiconductors do not correlate with their band gaps. The band gaps, approximated by values measured when the semiconductors are in contact with aqueous electrolyte at pH 1,[28] and the reactivities are as follows: TiO_2, 3.2 eV, most reactive; SnO_2, 3.8 eV, somewhat reactive; WO_3, 3.2 eV; unreactive; CdS, 2.5 eV, unreactive. Although the amount of light absorbed by the different semiconductors is not constant, the biggest factor in the different levels of effectiveness of the semiconductors in the aerobic reactions, given the complete lack of reactivity of all of them under anaerobic conditions, is not the inherent reactivities of their excited states to attack the substrate. Rather, it is the relative abilities of the various semiconductors to modulate the reactions of O_2 and O_2-derived oxidants including the chain-carrying peroxy radicals that are doubtless intermediates in the more active processes (i.e. those with TiO_2).

The reactive polyoxometalates in the presence of O_2 produce low yields of sulfoxide and sulfone and several unidentifiable products. More significantly, it is clear that many of the initial organic products are unstable under the reaction conditions, rendering the quantification of the organic products a marginally useful exercise. The nonacidic complexes $PMo_{12}O_{40}^{3-}$ and $PW_{12}O_{40}^{3-}$ lead to virtually no detectable removal of the thioether substrate under the brief conditions of irradiation used in the aerobic reactions (Table III). The reported lower level of reactivity of $PMo_{12}O_{40}^{3-}$ in the aerobic versus the anaerobic reactions derives from two experimental points—all the aerobic reactions were irradiated for shorter periods of time than their anaerobic counterparts (4 versus 16 h) and with lower energy light ($\lambda > 340$ nm versus $\lambda > 280$ nm = Pyrex cutoff). The isopolyoxotungstate, $W_{10}O_{32}^{4-}$, is the most effective system of all those evaluated under aerobic conditions, as it was under anaerobic conditions. The low toxicity of this and many other polyoxotungstates[29] and the accessibility of these materials in quantity from inexpensive starting materials suggest possible uses of these compounds in photocatalytic decontamination technology.

Acknowledgment. We thank the U.S. Army Research Office (Grant No. DAAL03-91-G-0021) for support of this work. We thank Yuqi Hou in our group for the sample of cubic WO_3.

(28) Reference 1d, pp 100-101.

(29) (a) Chermann, J. C.; Jasmin, C.; Mathe, G.; Raynaud, M. French Patent 58693/71. (b) Hill, C. L.; Hartnup, M.; Faraj, M.; Weeks, M.; Prosser-McCartha, C. M.; Brown, R. B.; Schinazi, R. F.; Sommadossi, J.-P. In *Advances in Chemotherapy of AIDS, Pharmacology and Therapeutics*; Diasio, R., Sommadossi, J.-P., Eds.; Pergamon: New York, 1990; pp 33-41. (c) Hill, C.; Weeks, M.; Schinazi, R. F.; *J. Med. Chem.* **1990**, *33*, 2767.

Contribution from the Chemistry Department, University of Kuwait, Box 5969, 13060 Safat, Kuwait, and Department of Chemistry, University of Helsinki, Et. Hesperiankatu 4, 00100 Helsinki, Finland

MS Xα Studies on the Colors of $BiPh_5$, $PbCl_6^{2-}$, and WS_4^{2-}: Are Relativistic Effects on the LUMO Important?

B. D. El-Issa,[†] P. Pyykkö,*[,‡] and H. M. Zanati[†]

Received June 21, 1990

Quasirelativistic multiple-scattering Xα (MS Xα) and pseudopotential Hartree–Fock calculations are performed on MX_5 (M = Bi, Sb; X=H, CCH) model systems in D_{3h} or C_{4v} site symmetries to elucidate the origin of the violet color of pentaphenylbismuth. The occurrence of this color only for Bi and for C_{4v} symmetry is related to the relativistic stabilization of the a_1 LUMO as concluded earlier from REX calculations. The nonrelativistic transitions are symmetry-forbidden. The relativistic perpendicular C_{4v} transition is allowed, in agreement with experiment. The study is extended further to include MS calculations on octahedral and tetrahedral site symmetries. The yellow color of $PbCl_6^{2-}$ is also attributed to the relativistic stabilization of the a_{1g} LUMO. The color difference between MoS_4^{2-} and WS_4^{2-} is mainly due to the shell-structure effects and not relativity.

1. Introduction

Pentaphenylbismuth was synthesized by Wittig and Clauss[1] in 1952. This compound shows an intense violet color, an unusual phenomenon for a main-group organometallic compound in its highest oxidation state. Seppelt et al.[2,3] have recently considered the origin of this color. They found that it never occurs in the lighter MR_5 congeners of Bi, such as Sb, and never occurs when the site symmetry of Bi is D_{3h}. Thus a necessary condition for this absorption is that the metal be bismuth and the site symmetry C_{4v}. A simple comparison of relativistic and nonrelativistic extended Hückel calculations on MH_5 model systems suggested that

* To whom correspondence should be addressed.
† University of Kuwait.
‡ University of Helsinki.

(1) Wittig, G.; Clauss, K. *Liebigs Ann. Chem.* **1952**, *578*, 136.
(2) Schmuck, A.; Buschmann, J.; Fuchs, J.; Seppelt, K. *Angew. Chem.* **1987**, *99*, 1206; *Angew. Chem., Int. Ed. Engl.* **1987**, *26*, 1180.
(3) Schmuck, A.; Pyykkö, P.; Seppelt, K. *Angew. Chem.* **1990**, *102*, 211; *Angew. Chem., Int. Ed. Engl.* **1990**, *29*, 213.

0020-1669/91/1330-2781$02.50/0

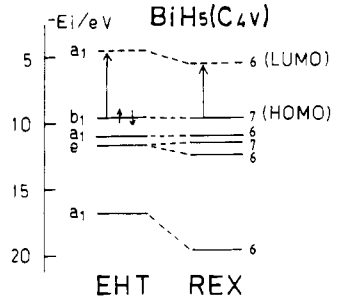

Figure 1. Comparison of relativistic and nonrelativistic extended Hückel (REX and EHT, respectively) orbital energies for $BiH_5(C_{4v})$. ζ_H = 1.3, α_H = −10 eV, Bi–H = 185 pm, and default bismuth parameters are given in the REX program.[28]

the absorption would be a HOMO–LUMO transition from a purely ligand b_1 HOMO to an antibonding a_1 LUMO having considerable bismuth 6s and 6p character. As a result of the relativistic 6s stabilization, these Bi orbitals are lowered in energy, not only the bonding MO's but also this empty, antibonding LUMO (see Figure 1 for the gist of the argument). Thus this color would be a conspicuous consequence of relativistic effects on an empty molecular orbital, a rather rare phenomenon. For D_{3h} symmetry, there are no empty coordination sites and this LUMO would still lie too high, despite its relativistic stabilization.

Furthermore the absorption is strongly polarized, only occurring for the electric field perpendicular to the molecular axis.[2,3] While these ideas are plausible, it is desirable to try to verify them with more fundamental methods, applied on more realistic model systems. We therefore here report multiple-scattering Xα (MS Xα) calculations on the original MH_5 systems for M = Sb, Bi, and the $Bi(CCH)_5$ system with a variable Bi–C bond distance. The two different geometries are considered and the role of relativity is studied by comparing quasirelativistic[4] and nonrelativistic calculations. The longest wavelength absorption bands in the octahedral complexes $SnCl_6^{2-}$ and $PbCl_6^{2-}$ and the tetrahedral complexes MoS_4^{2-} and WS_4^{2-} are also discussed, as other possible examples of the relativistic LUMO effect.

2. Method

The Multiple-scattering Xα method of Slater[5] and Johnson[6-8] was used for determining the electronic structure of the molecules under study.[9] This technique could be placed at the lower end of ab initio methods and is known to nicely reproduce the absorption energies of transition-metal complexes.[10-14] Some pseudopotential Hartree–Fock calculations using Gaussian 88[15] are also reported using the double-ζ "LANL1DZ" basis of Hay and Wadt.[16,17] The calculation parameters are reported in Table I. The exchange α values used for the atomic spheres are based on the values of Schwarz[18] while a weighted average was used for the inner- and the outer-sphere regions. The Norman criteria[19,20] were used for calculating the atomic sphere radii while the transition-state energies were calculated by employing the method of Slater.[21]

Table I. Assumed Geometries and Sphere Radii (au) for the Molecular Species MX_5, MX_6^{2-}, and MX_4^{2-},[a] with C_{4v} Bond Angles Put Equal to 90°

molecule	symmetry	sphere radius: outer sphere	sphere radius: M	M–X bond dist, pm
BiH_5	C_{4v}	5.099	2.828	185
BiH_5	D_{3h}	5.098	2.894	185
SbH_5	C_{4v}	4.927	2.754	177
SbH_5	D_{3h}	4.928	2.753	177
$Bi(CCH)_5$	C_{4v}	9.207	2.426	190
$Bi(CCH)_5$	C_{4v}	9.586	2.626	210
$Bi(CCH)_5$	C_{4v}	10.019	2.859	233
$Bi(CCH)_5$	D_{3h}	9.586	2.626	210
$SnCl_6^{2-}$	O_h	7.249	2.634	242
$PbCl_6^{2-}$	O_h	7.418	2.764	250
MoS_4^{2-}	T_d	6.705	2.463	217
WS_4^{2-}	T_d	7.418	2.545	219

[a] Exchange α values: Pb, 0.690 80; Sn, 0.700 78; Bi, 0.691 00; Sb, 0.700 55; Mo, 0.703 41; W, 0.693 17; S, 0.724 75; C, 0.759 28; H, 0.777 25.

Table II. Orbital and Transition-State Energies for the HOMO–LUMO Transition (eV) Where ΔE Stands for the Orbital Energy Difference and E_{trans} for the Transition-State Values with Pseudopotential HF Results Shown in Parentheses

case	type	E(HOMO)	E(LUMO)	ΔE	E_{trans}
$SbH_5(D_{3h})$	NR	−6.04	−1.35	4.69	4.69
	R	−5.92	−1.81	4.12	4.32
	(R	−8.82	+3.43	12.25)	
$SbH_5(C_{4v})$	NR	−6.19	−3.01	3.18	3.32
	R	−6.07	−3.12	2.95	3.07
	(R	−9.00	+0.44	9.44)	
$BiH_5(D_{3h})$	NR	−6.05	−1.40	4.65	4.87
	R	−5.71	−2.72	3.00	3.12
	(R	−8.61	+1.77	10.38)	
$BiH_5(C_{4v})$	NR	−6.16	−3.10	3.06	3.20
	R	−5.84	−3.52	2.31	2.38
	(R	−8.77	−0.01	8.76)	
$SnCl_6^{2-}(O_h)$	NR	−7.92	−3.67	4.24	4.37
	R	−7.86	−4.19	3.67	3.79
	(R	−3.66	+8.74	12.40)	
$PbCl_6^{2-}(O_h)$	NR	−7.99	−3.77	4.22	4.37
	R	−7.84	−5.09	2.75	2.79
	(R	−3.83	+6.55	10.38)	
$Bi(CCH)_5(D_{3h})$	NR	−9.81	−4.45	5.36	5.42
	R	−9.74	−6.15	3.59	3.62
	(R	−10.65	+2.51	13.16)	
$Bi(CCH)_5(C_{4v})$	NR	−9.82	−6.52	3.31	3.41
	R	−9.78	−7.55	2.23	2.31
	(R	−10.39	−0.46	9.93)	

The quasirelativistic hamiltonian used in ref 9 was first suggested by Cowan and Griffin.[22] Actually, its form already occurs in Dirac's first paper; see ref 23. It was introduced to MS calculations by Boring and Wood[24] and others[25] and was found to greatly refine the results in terms of the ordering of the orbitals and their respective composition. Due to relativistic effects, the orbitals that have preponderant s and p character are contracted and become more stable, in contrast to orbitals that have preponderant d and f character, which become more diffuse and less stable; see ref 26. To be exact, both $p_{3/2}$ and $d_{3/2}$ are borderline cases.

In this work, we focus on the longest wavelength absorption band in the model systems under study in a square-pyramidal (C_{4v} symmetry), a trigonal-bipyramidal (D_{3h} symmetry), an octahedral, and a tetrahedral

(4) Wood, J. H.; Boring, A. M. *Phys. Rev. B* **1978**, *18*, 2701.
(5) Slater, J. C. *Quantum Theory of Molecules and Solids*; McGraw-Hill: New York, 1974; Vol. IV.
(6) Johnson, K. H. *Int. J. Quantum Chem., Symp.* **1967**, *1S*, 361.
(7) Johnson, K. H. *Int. J. Quantum Chem.* **1967**, *4*, 153.
(8) Johnson, K. H. *Adv. Quantum Chem.* **1973**, *7*, 143.
(9) Cook, M.; Case, D. *QCPE* **1982**, *14*, No. 465.
(10) King, C.; Wang, J.; Khan, N.; Fackler, J. P., Jr. *Inorg. Chem.* **1989**, *28*, 2145.
(11) Morin, M.; Salahub, D. R.; Nour, S.; Mehadji, C.; Chermette, H. *Chem. Phys. Lett.* **1989**, *159*, 472.
(12) Cotton, F. A.; Feng, X.; Matusz, M.; Poli, R. *J. Am. Chem. Soc.* **1988**, *110*, 7077.
(13) Goursot, A.; Chermette, H.; Waltz, W. L.; Lilie, J. *Inorg. Chem.* **1989**, *28*, 2241.
(14) El-Issa, B. D.; Ali, A. A. M.; Zanati, H. *Inorg. Chem.* **1989**, *28*, 3297.
(15) Frisch, M. J.; Head-Gordon, M.; Schlegel, H. B.; Raghavachari, K.; Binkley, J. S.; Gonzalez, C.; Defrees, D. J.; Fox, D. J.; Whiteside, R. A.; Seeger, R.; Melius, C. F.; Baker, J.; Martin, R.; Kahn, L. R.; Stewart, J. J. P.; Fluder, E. M.; Topiol, S.; Pople, J. A. *Gaussian 88*; Gaussian Inc.: Pittsburgh, PA, 1988.
(16) Hay, P. J.; Wadt, W. R. *J. Chem. Phys.* **1985**, *82*, 270.
(17) Wadt, W. R.; Hay, P. J. *J. Chem. Phys.* **1985**, *82*, 284.
(18) Schwarz, K. *Phys. Rev. B* **1972**, *B5*, 2466.
(19) Norman, J. G., Jr. *J. Chem. Phys.* **1974**, *61*, 4630.
(20) Norman, J. G., Jr. *Mol. Phys.* **1976**, *31*, 1191.
(21) Slater, J. C. *Adv. Quantum Chem.* **1972**, *6*, 1.
(22) Cowan, R. D.; Griffin, D. C. *J. Opt. Soc. Am.* **1976**, *66*, 1010.
(23) Pyykkö, P. *Relativistic Theory of Atoms and Molecules*; Lecture Notes in Chemistry 41; Springer: Berlin, 1986; p 13.
(24) Boring, M.; Wood, J. H. *J. Chem. Phys.* **1979**, *71*, 32, 392.
(25) Reference 23, Table 7.6.
(26) Pyykkö, P. *Chem. Rev.* **1988**, *88*, 563.

Table III. Relativistic Orbital Energies (rydbergs) and Composition of the BiH_5 Orbitals under C_{4v} Symmetry[a]

		Bi					
	E	s	p	d	f	H_{eq} s	H_{ax} s
$4a_1$*	−0.259	0.121	0.102	0.198	0.002	0.139	0.020
$2b_1$	−0.429			0.223	0.000	0.194	
$3a_1$	−0.606	0.008	0.362	0.052	0.017	0.012	0.514
2e	−0.700		0.394	0.000	0.030	0.142	
$2a_1$	−1.173	0.755	0.003	0.001	0.001	0.046	0.055
tot. pop.		1.520	2.310	10.480	0.160	1.090	1.152
tot. pop.		(1.592	2.600			1.170	1.125)

[a] An $l_{max} = 3$ was used for Bi. H_{eq} and H_{ax} stand for equatorial and axial hydrogens, respectively. MS and pseudopotential populations (in parentheses) are also included. The LUMO is indicated by an asterisk.

environment using a relativistic (R) and a nonrelativistic (NR) Hamiltonian. In order to further understand the relativistic stabilization of the LUMO, minimal and extended bases will be employed around the metal and the ligand centers. It could be added that only the HF occupied MO energies and the MS Xα excitation energies are physically meaningful. The trends of the HF virtual MO and all MS Xα orbital energies are of more qualitative interest. So are the comparisons of LCAO and MS population. In practice, the orbital-energy differences, ΔE, and the transition-state energies, E_{trans}, are quite similar, making attribution to the LUMO meaningful. In all cases, the molecular geometries have been fixed.

3. Results and Discussion

3.1. MH_5 Models. In Table II, we summarize the results obtained for the pentahydride models in which M = Bi or Sb. In this table, we report the relativistic (R) and nonrelativistic (NR) MS orbital energies of the HOMO and LUMO, the HOMO–LUMO gap, and the longest wavelength transition-state energy in both a C_{4v} and a D_{3h} environment. We also report in the table Gaussian 88 pseudopotential HF calculations.

The MS orbital energies and the corresponding composition of the valence orbitals are reported for the relativistic case (Table III). We also include in Table III MS and pseudopotential Mulliken populations. Since an $l_{max} = 3$ was used around Bi, the composition includes contributions from the s, p, d, and f bases. The HOMO is $2b_1$ which contains contributions from the d bases of Bi in addition to contributions from the equatorial hydrogens while the LUMO is $4a_1$ and contains appreciable contributions from the s, p, and d bases of Bi in addition to contributions from the two sets of hydrogens. As seen from Tables III and IV, the orbital-energy-difference and transition-state results for the HOMO–LUMO excitation are closely similar. The relativistic change, from 3.20 to 2.38 eV for $l_{max} = 3$, is mainly due to the relativistic stabilization of the LUMO, as originally expected. The HOMO suffers a small destabilization. The driving force is the 6s character of the LUMO. (For a closer analysis of direct and indirect relativistic effects on various atomic shells, see Schwarz et al.[27].)

In order to study the effect of the inclusion of d partial waves around Bi, the calculations were repeated with only valence s and p waves ($l_{max} = 1$) used around that center. The two sets of results are summarized in Table IV. The relativistic HOMO–LUMO gap is calculated to be 2.013 and 2.313 eV for the $l_{max} = 1$ and the $l_{max} = 3$ cases, respectively, while the corresponding nonrelativistic values are calculated to be 2.762 and 3.061 eV. The inclusion of the d and f partial waves thus increases the gap by 0.30 eV in both cases (R and NR). Relativistic effects are seen to diminish the gap by 0.75 eV for both l_{max} values. The corresponding decrease from EHT to REX[28] was also 0.77 eV. For the $l_{max} = 1$ case, the MS population is calculated to be Bi (6s = 1.54; 6p = 2.57), close to the pseudopotential population of Bi (6s = 1.59; 6p = 2.60).

3.1.1. BiH_5 in a D_{3h} Environment. The inclusion of d bases around the Bi in the D_{3h} environment has produced results similar to the C_{4v} ones and hence the results reported in Table V are those for the two cases in which l_{max} around Bi was taken as 1. The HOMO in this case is $2a_1'$ and involves contributions from the hydrogen s bases while the LUMO, which is $3a_1'$, has appreciable Bi s character and does not contain any Bi p bases by symmetry. Note that the D_{3h} HOMO and LUMO both belong to a_1' although the HOMO has no 6s character. This can be understood in a minimal (H_{ax}, H_{eq}, 6s) a_1' basis as a special case of the Hamiltonian[29-31]

$$H = \begin{pmatrix} \alpha_{1s} & 0 & a \\ 0 & \alpha_{1s} & b \\ a & b & \alpha_{6s} \end{pmatrix}$$

leading to a pure 1s level between 1s–6s bonding and antibonding ones. The relativistic stabilization of the LUMO is calculated to be 1.347 eV while the destabilization of the HOMO, from NR to R, is calculated to be 0.204 eV. As the $2a_1'$ HOMO has no Bi contributions, this effect must be an indirect one, analogous to the indirect destabilization of d or f atomic orbitals. The HOMO–LUMO gap for the $l_{max} = 1$ case is calculated to be 2.530 eV for the relativistic case as compared to the nonrelativistic value of 4.081 eV. The relativistic decrease of this gap is 1.55 eV as compared to 0.749 eV for the C_{4v} model system. The larger relativistic stabilization of the LUMO, 1.143 and 0.381 eV for the D_{3h} and C_{4v} model systems, respectively, may be intuitively understood since, in the D_{3h} model, the present composition of the Bi s bases in the LUMO that are responsible for the relativistic stabilization is appreciably larger than in the corresponding C_{4v} model (23% as compared to 14%).

3.1.2. Comparison of the Pentahydride Systems in the Two Model Environments. Because of the higher symmetry of the D_{3h} model, the antibonding (6s, 6p) interactions of Bi with the equatorial and axial hydrogens lead to a larger HOMO–LUMO gap in the D_{3h} model as compared to that of the C_{4v} counterpart. Although large, the relativistic stabilization of the LUMO is not sufficient to place the longest wavelength transition in the lower energy end of the visible spectrum. Schmuck et al.[2] report an absorption in the green-yellow region at 532 nm or 2.33 eV for pentaphenylbismuth. In the case of the C_{4v} model, the antibonding and the relativistic factors are less marked and, as our calculations show, the HOMO–LUMO excitation energy of $BiH_5(C_{4v})$ would be expected to occur in the visible region. The symmetry aspects[32] of the HOMO–LUMO transitions are considered in Table VI. It is seen that nonrelativistically all transitions are forbidden while relativistically the C_{4v} x,y one (electrical field perpendicular to the highest-fold symmetry axis) is allowed, containing Γ_1 (Bethe notation for a_1), in agreement with experiment. It is also clear that the longest wavelength transition in both D_{3h} prototypes (R and NR) remains forbidden. Thus the lack of color in the D_{3h} bismuth compounds would already be explained by relativistic symmetry alone. The transitions, discussed below for octahedral and tetrahedral symmetries, are allowed.

Actually, the highest symmetry that pentaphenyl bismuth could have is C_{2v}. In that double group, all relativistic MOs belong to the same irreducible representation and all transitions are, in principle, allowed. In practice the effects of low symmetry, due to remote groups, may not be large.

3.1.3. SbH_5 Model Systems. In Table II, we also report the MS orbital energies and the HOMO–LUMO excitation energy for the relativistic and nonrelativistic calculations on the SbH_5 model system in a C_{4v} environment. In these calculations, an $l_{max} = 3$ was used around Sb in order to quantify the relativistic stabilization of the LUMO. The s, p, and d bases of Sb in the LUMO ($4a_1$) are all populated, and the apparent stabilization

(27) Schwarz, W. H. E.; van Wezenbeek, E. M.; Baerends, E. J.; Snijders, J. G. *J. Phys. B: At. Mol. Opt. Phys.* **1989**, *22*, 1515.
(28) Pyykkö, P. *Methods Comput. Chem.* **1988**, *2*, 137.
(29) Burdett, J. K. *Prog. Solid State Chem.* **1984**, *15*, 241.
(30) Hoffmann, R.; Li, J.; Wheeler, R. A. *J. Am. Chem. Soc.* **1987**, *109*, 6600.
(31) Boerrigter, P. M.; Snijders, J. G.; Dyke, J. M. *J. Electron Spectrosc. Relat. Phenom.* **1988**, *46*, 43.
(32) Koster, G. F.; Dimmock, J. O.; Wheeler, R. G.; Statz, H. *Properties of the Thirty-Two Point Groups*; MIT Press: Cambridge, MA, 1963.

Table IV. Analysis of the HOMO and LUMO Relativistic and Nonrelativistic Results of BiH_5 Using an $l_{max} = 1$ and $l_{max} = 3$ around Bi in a C_{4v} Environment

	relativistic		nonrelativistic	
	$l_{max} = 1$	$l_{max} = 3$	$l_{max} = 1$	$l_{max} = 3$
LUMO, Ry	−0.291	−0.259	−0.250	−0.228
	Bi(0.14, 0.09)	Bi(0.12, 0.10, 0.20, 0.00)	Bi(0.09, 0.24)	Bi(0.08, 0.22, 0.00, 0.00)
HOMO, Ry	−0.440	−0.429	−0.453	−0.453
	Bi(*b*, *b*)	Bi(*b*, *b*, 0.22, 0.00)	Bi(*b*, *b*)	Bi(*b*, *b*, 0.23, 0.00)
HOMO–LUMO gap, eV	2.013	2.313	2.762	3.061
HOMO–LUMO excitation, eV	2.107	2.380	2.894	3.200
stabilization energy of LUMO, eV	0.558	0.422		
destabilization energy of HOMO, eV	0.177	0.326		
MS pop.	Bi(1.54, 2.57)	Bi(1.52, 2.31, 10.48, 0.16)	Bi(1.33, 2.51)	Bi(1.30, 2.20, 10.52, 0.17)
Gaussian pop.	Bi(1.59, 2.60)			

[a] Composition of the orbitals are only for Bi and read (s, p) for $l_{max} = 1$ and (s, p, d, f) for $l_{max} = 3$. Also included is the MS and Gaussian 88 population of the Bi 6s and 6p orbitals. [b] Zero contribution.

Table V. Relativistic (a) and Nonrelativistic (b) Orbital Energies in (rydbergs) and the Corresponding Orbital Composition for BiH_5 in a D_{3h} Environment[a]

		Bi			
	E	s	p	H_{eq} s	H_{ax} s
		(a) Relativistic			
$3a_1'$*	−0.237	0.228		0.155	0.153
$2a_1'$	−0.423	0.000		0.132	0.301
1e′	−0.712		0.419	0.194	
$1a_2''$	−0.728		0.439		0.280
$1a_1'$	−1.234	0.770		0.047	0.044
tot. pop.		1.540	2.554	1.134	1.250
tot. pop.		(1.578	2.455	1.165	1.236)
		(b) Nonrelativistic			
$3a_1'$*	−0.138	0.253		0.155	0.141
$2a_1'$	−0.438	0.000		0.130	0.305
1e′	−0.724		0.408	0.197	
$1a_2''$	−0.740		0.430		0.285
$1a_1'$	−1.091	0.666		0.069	0.064
tot. pop.		1.332	2.492	1.186	1.308

[a] An $l_{max} = 1$ was used around Bi. The MS and Gaussian 88 pseudopotential (in parentheses) populations are also included. H_{eq} and H_{ax} stand for equatorial and axial hydrogens, respectively. The LUMO is indicated by an asterisk.

Table VI. Symmetry Properties of the Transition Matrix Element ⟨HOMO|*r*|LUMO⟩ with the Relativistic Bethe Notation of Koster et al.[32] Used

case	group	HOMO	LUMO	*r*	product of irreps
NR	C_{4v}	b_1	a_1	*x*,*y* (e)	e
				z (a_1)	b_1
	D_{3h}	a_1'	a_1'	*x*,*y* (e′)	e′
				z (a_2'')	a_2''
R	C_{4v}	Γ_7	Γ_6	*x*,*y* (Γ_5)	$\Gamma_1 + \Gamma_2 + \Gamma_3 + \Gamma_4 + 2\Gamma_5$
				z (Γ_1)	$\Gamma_3 + \Gamma_4 + \Gamma_5$
	D_{3h}	Γ_7	Γ_7	*x*,*y* (Γ_6)	$\Gamma_3 + \Gamma_4 + \Gamma_5 + 2\Gamma_6$
				z (Γ_4)	$\Gamma_3 + \Gamma_4 + \Gamma_6$

(0.1 eV) is seen to slightly dominate. The HOMO ($2b_1$) does not contain any contributions from the s and p bases on Sb by symmetry, and its destabilization is calculated to be 0.12 eV. The HOMO–LUMO excitation energy is calculated to be 3.065 eV for the relativistic case and 3.322 eV for the nonrelativistic counterpart. Relativistic corrections for Sb are thus not sufficient to reduce the HOMO–LUMO gap to the lower energy end of the visible spectrum.

For the D_{3h} model, the relativistic stabilization of the LUMO is rather large due to the appreciable population of the Sb 5s basis (20% composition). The relativistic HOMO–LUMO excitation energy is calculated to be 4.321 eV as compared to 4.958 eV for the nonrelativistic counterpart. Neither of these values correspond to absorption in the visible region and the conclusion is that the SbH_5 model system in a D_{3h} environment would be expected to exhibit no color. The appreciably larger HOMO–LUMO gap in the SbH_5 models as compared to the corresponding BiH_5 counterparts may therefore be attributed to smaller relativistic effects and greater antibonding interactions in the LUMO.

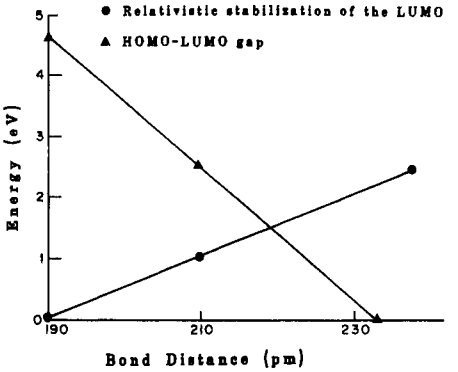

Figure 2. HOMO–LUMO gap and the relativistic stabilization of the LUMO (eV) vs the Bi–C bond distance (pm) in $Bi(CCH)_5$.

3.2. Pentaacetylide Model Systems. As a more realistic model system, we replaced the –H ligand by –CCH, a system with multiply bonded carbon. A Bi–C distance of 233 pm, which is equal to that in pentaphenylbismuth[3] was first used. Such a distance, however, resulted in an almost degenerate HOMO and LUMO in the case of a C_{4v} model and an unrealistic stabilization of the LUMO in the case of the D_{3h} prototype. As the bonding and antibonding interactions between the Bi and the ligands are very much dependent on the Bi–L distance, the calculations were also performed for Bi–C distances of 210 and 190 pm. The latter case corresponds to an underestimated distance in which strong antibonding interactions are expected to increase the HOMO–LUMO gap. The LUMO in such a case was determined to lose much of its Bi s character with the obvious result of an almost negligible relativistic stabilization. In Figure 2, we show a plot of the HOMO–LUMO gap and the corresponding relativistic stabilization of the LUMO vs the Bi–C distance for the pentaacetylide model in a C_{4v} environment. It is obvious that a distance of 210 pm is capable of producing a relativistic HOMO–LUMO gap that would place the longest wavelength absorption band in the visible region. This distance, in fact, is comparable with the Bi–C distance in analogous compounds[33,34] and will therefore be used for the pentaacetylide models in the discussion to follow. No attempt was made to find total energy minima for any of the present systems.

(33) Wells, A. F. *Structural Inorganic Chemistry*, 5th. Ed.; Clarendon: Oxford, England 1984. A Bi–C distance of 227 pm is quoted for $Bi(CH_3)_3$ on p 879.

(34) Ali, M.; McWhinnie, W. R.; West, A. A.; Hamor, T. A. *J. Chem. Soc., Dalton Trans.* **1990**, 899. Bi–C distances of 224–226 pm are quoted for phenyl groups.

Table VII. Comparison between the Relativistic and Nonrelativistic Orbital Energies (rydbergs) and the HOMO–LUMO Gap for $Bi(CCH)_5$ under C_{4v} Symmetry

	relativistic				nonrelativistic			
		Bi				Bi		
	E	s	p	d	*E*	s	p	d
$9a_1$	−0.555	0.171	0.117	0.088	−0.479	0.147	0.242	0.134
$1a_2$	−0.719				−0.722			
7e	−0.728		0.000	0.000	−0.734		0.000	0.001
6e	−0.738		0.001	0.000	−0.741		0.001	0.000
$5b_1$	−0.738			0.000	−0.755			0.000
$8a_1$	−0.750	0.002	0.001	0.025	−0.755	0.002	0.003	0.024
5e	−0.770		0.000	0.018	−0.777		0.000	0.020
$2b_2$	−0.778			0.025	−0.784			0.027
$4b_1$	−0.867			0.174	−0.898			0.177
$7a_1$	−1.054	0.009	0.304	0.056	−1.062	0.011	0.270	0.065
4e	−1.162		0.379	0.000	−1.164		0.368	0.000
$6a_1$	−1.250	0.000	0.000	0.000	−1.250	0.000	0.000	0.000
$3b_1$	−1.250			0.000	−1.250			0.000
3e	−1.251		0.000	0.000	−1.251		0.000	0.000
$5a_1$	−1.263	0.000	0.000	0.000	−1.267	0.000	0.000	0.000
$4a_1$	−1.677	0.730	0.004	0.001	−1.520	0.608	0.001	0.002

HOMO/LUMO gap = 2.31 (R), 3.306 eV (NR)

HOMO–LUMO excitation energy = 2.310 (R), 3.410 eV (NR)

3.2.1. $Bi(CCH)_5$ in a C_{4v} Environment. In Table VII, we summarize the relativistic and nonrelativistic orbital energies of $Bi(CCH)_5$ in a C_{4v} environment in which partial waves up to an $l_{max} = 2$ were used around Bi. The charge composition in that table includes contributions from only Bi s, p, and d bases while the dashes signify no contribution of these bases by symmetry. The $9a_1$ LUMO and the $4a_1$ orbitals contain appreciable contributions from the Bi s bases and are thus seen to be relativistically stabilized. The former, however, is also seen to include contributions from the p_z and d_{z^2} bases of Bi. Orbitals that contain large contributions from the Bi p bases, namely 4e and $7a_1$, nonetheless are seen to be slightly destabilized. The Bi d base contribution is rather large in the $4b_1$ orbital, which represents bonding interactions between the sp hybrid orbitals of the C atoms and the $Bi(d_{x^2-y^2})$ basis. The HOMO is a pure π orbital centered on the two C atoms of the acetyl ligands and is consequently seen to be slightly affected. The relativistic and nonrelativistic HOMO–LUMO gaps are calculated to be 2.231 and 3.306 eV, respectively, while the corresponding HOMO–LUMO transition-state energies are calculated to be 2.310 and 3.410 eV. A contour representation of the HOMO and LUMO wave functions is shown in Figure 3. In order to further investigate the effect of the Bi bases in determining the energy gap between the HOMO and the LUMO, the calculations were repeated by using an $l_{max} = 1$ around Bi. A comparison between the relativistic and nonrelativistic results concerning the HOMO and the LUMO for two cases in which $l_{max} = 1$ or 2 around Bi is summarized in Table VIII. It is interesting to note that the inclusion of d partial waves around Bi results in a smaller HOMO–LUMO gap as compared with the $l_{max} = 1$ case. In both the relativistic and the nonrelativistic calculations, the inclusion of d partial waves around Bi are seen to result in a slight destabilization of the HOMO. The relativistic LUMO, however, is seen to be slightly affected by the inclusion of d partial waves in contrast with the nonrelativistic calculation.

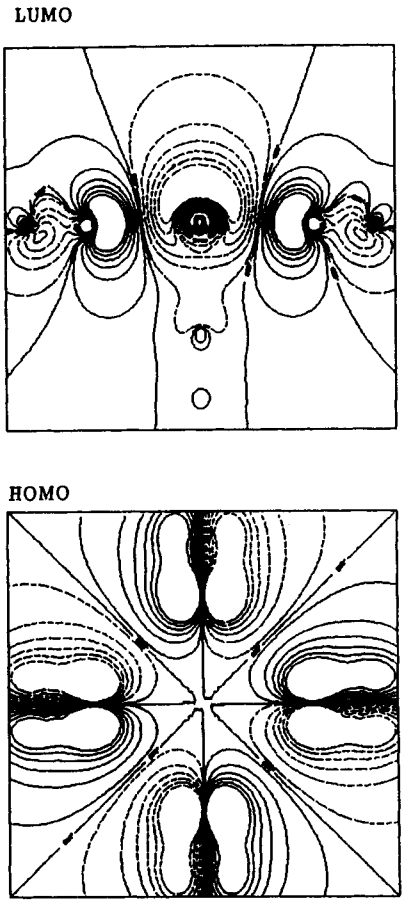

Figure 3. Wave function representations of the LUMO and HOMO in $Bi(CCH)_5$ under C_{4v} symmetry. Contour levels are taken every 0.06 units. The HOMO is shown in the *xy* plane and the LUMO in the *xz* plane, *z* being the molecular axis.

3.2.2. $Bi(CCH)_5$ in a D_{3h} Environment. In Table IX we summarize results obtained for pentaacetyl bismuth in a D_{3h} environment. The LUMO in this case does not contain any Bi p character and is again seen to be relativistically stabilized. Except for the $7a_1'$ orbital, contributions from the Bi d bases are seen to be minimal. The HOMO is the doubly degenerate 3e″ orbital and represents π interactions on the acetyl moieties. The relativistic HOMO–LUMO gap is calculated to be 3.592 eV as compared to the nonrelativistic value of 5.360 eV while the respective HOMO–LUMO transition state energies are calculated to be 3.62 and 5.42 eV. As in the case of the pentahydride models, the large HOMO–LUMO separation in the D_{3h} as compared with the C_{4v} model system may be attributed to the strong antibonding

Table VIII. Analysis of the HOMO and LUMO Relativistic and Nonrelativistic Results, Using $l_{max} = 1$ and $l_{max} = 2$ around Bi in $Bi(CCH)_5$ in a C_{4v} Environment[a]

	relativistic		nonrelativistic	
	$l_{max} = 1$	$l_{max} = 2$	$l_{max} = 1$	$l_{max} = 2$
LUMO, Ry	−0.558	−0.555	−0.468	−0.479
	Bi(0.18, 0.09)	Bi(0.17, 0.12, 0.09)	Bi(0.16, 0.21)	Bi(0.15, 0.24, 0.13)
HOMO, Ry	−0.732	−0.719	−0.735	−0.722
	Bi(*b*, *b*)	Bi(*b*, *b*, *b*)	Bi(*b*, *b*)	Bi(*b*, *b*, *b*)
HOMO–LUMO gap, eV	2.367	2.231	3.632	3.306
stabilization energy of LUMO, eV	1.224	1.034		
destabilization energy of HOMO, eV	0.041	0.041		
MS pop.	Bi(1.52, 2.29)	Bi(1.48, 2.14, 10.53)	Bi(1.29, 2.23)	Bi(1.24, 2.04, 10.60)
Gaussian 88 pop.	Bi(1.49, 1.82)			

[a] Composition of the orbitals are only for Bi and read (s, p) for $l_{max} = 1$ and (s, p, d) for $l_{max} = 2$. Also included is the MS and Gaussian 88 pseudopotential populations. [b] Zero contribution

Table IX. Analysis of the HOMO and LUMO Relativistic and Nonrelativistic Results, Using l_{max} = 1 and l_{max} = 2 around Bi in $Bi(CCH)_5$ in a D_{3h} Environment[a]

	relativistic		nonrelativistic	
	l_{max} = 1	l_{max} = 2	l_{max} = 1	l_{max} = 2
LUMO, Ry	−0.485	−0.452	−0.349	−0.327
	Bi(0.25, *b*)	Bi(0.25, *b*, 0.00)	Bi(0.24, *b*)	Bi(0.23, *b*, 0.01)
HOMO, Ry	−0.729	−0.716	−0.735	−0.721
	Bi(*b*, *b*)	Bi(*b*, *b*, 0.00)	Bi(*b*, *b*)	Bi(*b*, *b*, 0.00)
HOMO–LUMO gap, eV	3.320	3.592	5.252	5.360
stabilization energy of LUMO, eV	1.850	1.701		
destabilization energy of HOMO, eV	0.082	0.068		
MS pop.	Bi(1.51, 2.31)	Bi(1.48, 2.15, 10.54)	Bi(1.30, 2.25)	Bi(1.26, 2.06, 10.61)
Gaussian 88 pop.	Bi(1.53, 1.65)			

[a] Composition of the orbitals are only for Bi and read (s, p) for l_{max} = 1 and (s, p, d) for l_{max} = 2. Also included is the MS and Gaussian 88 pseudopotential populations. [b] Zero contribution.

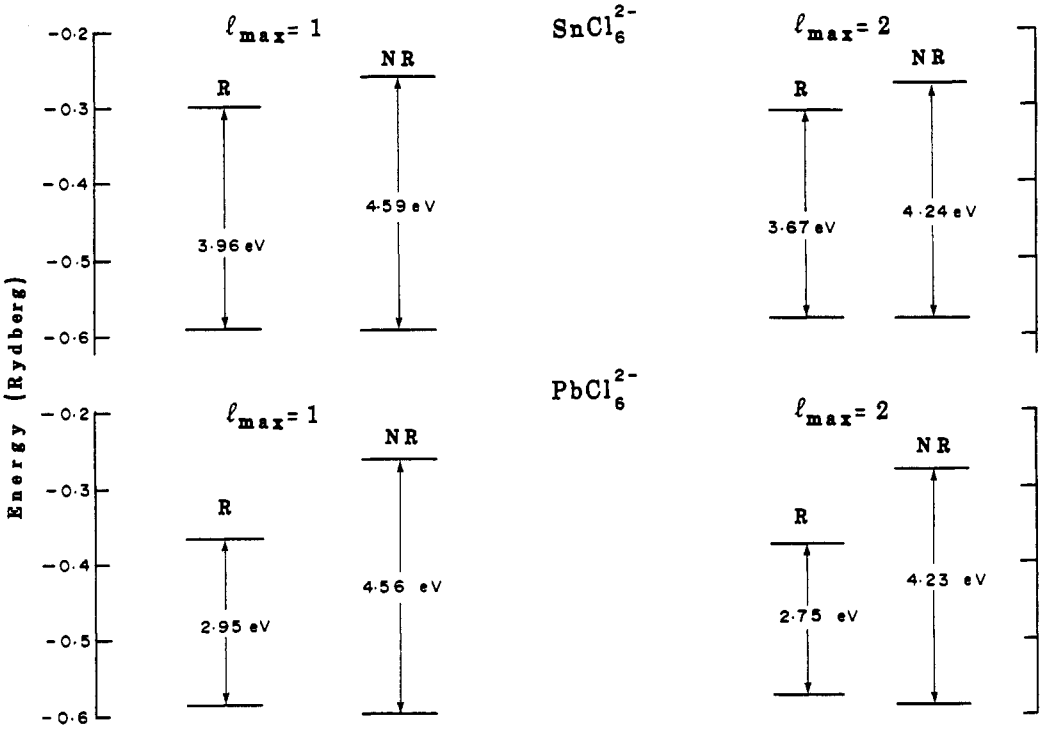

Figure 4. Relativistic and nonrelativistic HOMO–LUMO gap (eV) for l_{max} = 1 or 2 around Sn and Pb in the octahedral site symmetries of $SnCl_6^{2-}$ and $PbCl_6^{2-}$.

interactions between the Bi and the ligand moieties. In Table IX, we also compare the results obtained for this model in which l_{max} around Bi was taken as 1 or 2. The relativistic stabilization of the LUMO is again seen to decrease the HOMO–LUMO gap to 3.320 and 3.592 eV for the two cases in which l_{max} = 1 and 2, respectively. In contrast to the C_{4v} model, the inclusion of d partial waves around Bi is seen to result in a greater separation between the HOMO and the LUMO. In neither of these cases, however, are relativistic effects seen to be sufficient to place the longest wavelength absorption band in the visible region.

3.3. Octahedral and Tetrahedral Models. As further examples of colors possibly due to relativistic effects on the final state (LUMO) of the optical absorption, we consider $PbCl_6^{2-}$ and WS_4^{2-} and their lighter analogues. In these two cases, a stabilization of the Pb 6s a_1* and a destabilization of the W 5d LUMO could be expected.[26] The parameters used in the MS calculations are reported in Table I.

In Table X, the relativistic and nonrelativistic orbital energies of $PbCl_6^{2-}$ are reported for l_{max} = 2 around Pb and Cl. The table also includes the HOMO–LUMO gap as well as the calculated first allowed excitation energies. The HOMO in this case consists of pure p bases around the Cl ligands. Such an orbital, therefore, is not expected to be affected by direct relativistic corrections. The relativistic effects, however, are quite significant in the LUMO, which contains a considerable contribution from the Pb basis. In fact, the energy of the HOMO suffers a slight relativistic destabilization (0.122 eV) while the energy of the LUMO is seen to be relativistically stabilized by 1.320 eV. The relativistic HOMO–LUMO gap is calculated to be 2.748 eV as compared

Table X. Comparison between the Relativistic and Nonrelativistic Orbital Energies (rydbergs) and the HOMO–LUMO Gap for $PbCl_6^{2-}$ in an Octahedral Environment in Which l_{max} = 2 for Pb and Cl

	relativistic	nonrelativistic	
$3a_{1g}$	−0.374	−0.277	LUMO
$1t_{1g}$	−0.579	−0.588	HOMO
$3e_g$	−0.576	−0.596	
$3t_{1u}$	−0.604	−0.613	
$1t_{2u}$	−0.610	−0.620	
$2t_{2g}$	−0.659	−0.671	
$2t_{1u}$	−0.734	−0.744	
$2a_{1g}$	−1.059	−0.956	
$2e_g$	−1.445	−1.463	
$1t_{1u}$	−1.482	−1.491	
$1a_{1g}$	−1.539	−1.535	
$1t_{2g}$	−1.761	−2.013	
$1e_g$	−1.791	−2.032	
HOMO–LUMO gap	0.202 Ry	0.311 Ry	
	2.748 eV	4.231 eV	
first allowed transition ($t_{1u} \rightarrow a_{1g}$)	3.197 eV	4.694 eV	

Table XI. Analysis of the HOMO and LUMO Relativistic and Nonrelativistic Results, Using $l_{max} = 1$ and $l_{max} = 2$ around Pb and Cl in an Octahedral Environment[a]

	relativistic		nonrelativistic	
	$l_{max} = 1$	$l_{max} = 2$	$l_{max} = 1$	$l_{max} = 2$
LUMO, Ry	−0.368	−0.374	−0.262	−0.277
	Pb(0.26, *b*)	Pb(0.23, *b*, *b*)	Pb(0.39, *b*)	Pb(0.33, *b*, *b*)
HOMO, Ry	−0.585	−0.576	−0.597	−0.588
	Pb(*b*, *b*)	Pb(*b*, *b*, 0.072)	Pb(*b*, *b*)	Pb(*b*, *b*, *b*)
HOMO–LUMO gap, eV	2.952	2.748	4.558	4.231
first allowed transition ($3t_{1u} \rightarrow 3a_{1g}$), eV	3.442	3.197	5.115	4.694
stabilization energy of LUMO, eV	1.442	1.320		
destabilization energy of HOMO, eV	0.163	0.122		
MS pop.	Pb(1.35, 1.40)	Pb(1.33, 1.41, 10.25)	Pb(1.06, 1.38)	Pb(1.04, 1.38, 10.31)
Gaussian 88 pop.	Pb(1.22, 1.39)			

[a] Composition of the orbitals are only for Pb and read (s, p) for $l_{max} = 1$ and (s, p, d) for $l_{max} = 2$. Also included is the lead MS and the Gaussian 88 pseudopotential populations.

to the unrelativistic value of 4.231 eV while the corresponding allowed longest wavelength transitions ($3t_{1u} \rightarrow 3a_{1g}$) are calculated to be 3.197 and 4.694 eV. We note here that the HOMO–LUMO transition is parity forbidden. The consequence of using a relativistic Hamiltonian and an $l_{max} = 2$ around Pb and Cl seems to result in a decrease of the first allowed excitation energy in a manner that would place such an excitation in the highest energy end of the visible spectrum (Table XI). These results are consistent with the observation that $PbCl_6^{2-}$ salts are colored while the $SnCl_6^{2-}$ congeners are colorless.[35] The optical absorption of $PbCl_6^{2-}$ actually has its maximum at 4.04 eV, in the UV region and is assigned to the allowed $t_{1u} \rightarrow a_{1g}$ transition by Jørgensen.[35] This is a little larger than our calculated transition-state energy (Table XI). The essential point is that, without the relativistic stabilization of the $PbCl_6^{2-}$ a_{1g} LUMO, it would lie 1.32 eV higher and the visible tail would disappear. The frontier orbital energies of both $SnCl_6^{2-}$ and $PbCl_6^{2-}$ are summarized in Figure 4.

Cases in which the LUMO is relativistically destabilized occur in transition-metal complexes in which the LUMO contains significant contributions from the transition metal d bases while the HOMO is of pure ligand character. The relativistic longest wavelength excitation energy of tetrahedral complexes, such as MoS_4^{2-} and WS_4^{2-}, are calculated to be 2.76 and 3.54 eV, respectively (see Table I for the assumed geometries). These values are to be compared with the corresponding experimental values of 2.65 and 3.16 eV.[36,37] The experimental difference between the absorption bands is 0.51 eV while the corresponding relativistic and nonrelativistic differences are 0.78 and 0.61 eV. If the color difference between the two compounds would be of relativistic origin, the NR difference should approach zero. In our model, for the free MS_4^{2-} groups, it is only reduced by 0.17 eV, of the total experimental difference of 0.51 eV. Thus relativistic effects are not the main reason for the color difference in this case, contrary to the conjecture of Pyykkö.[26]

4. Conclusion

In the two cases, BiL_5 and $PbCl_6^{2-}$, where the expected relativistic effect is the stabilization of an a_1^* LUMO, containing metal 6s character, the present answer to the title question is "yes". This supports the earlier conclusion[2] based on REX calculations on BiH_5 models.

In the third case, WS_4^{2-}, where the expected[26] relativistic effect was the destabilization of a LUMO, containing metal 5d character, the answer rather is "no". This raises the general theoretical question: Why are relativistic MO stabilizations large and roughly proportional to the heavy-metal s character but the destabilizations, in a case like the WS_4^{2-} LUMO, much smaller than expected from their 5d character?

Acknowledgment. B.D.E.-I. would like to express his gratitude to the Research Management Unit at Kuwait University for supporting this work (Project SC044). We also thank the reviewers for their comments.

(35) Jørgensen, C. K. *Adv. Chem. Phys.* **1963**, *5*, 30.
(36) Jostes, R.; Müller, A.; Diemann, E. *J. Mol. Struct.: THEOCHEM* **1986**, *137*, 311.
(37) Müller, A.; Diemann, E.; Jostes, R.; Bögges, H. *Angew. Chem.* **1981**, *93*, 957.